

TIME REVERSAL FOCUSING OF HIGH AMPLITUDE SOUND IN A REVERBERATION
CHAMBER

Matthew L. Willardson

Physics 492R Capstone Report submitted to the faculty of
Brigham Young University
in partial fulfillment of the requirements for the degree of

Bachelor of Science

Brian E. Anderson, Advisor

Department of Physics and Astronomy

Brigham Young University

August 2017

Copyright © 2017 Matthew L. Willardson

All Rights Reserved

ABSTRACT

TIME REVERSAL FOCUSING OF HIGH AMPLITUDE SOUND IN A REVERBERATION CHAMBER

Matthew L. Willardson

Department of Physics and Astronomy

Bachelor of Science

Time reversal (TR) is a signal processing technique that can be used for intentional sound focusing. While it has been studied in room acoustics, the application of TR to produce a high amplitude focus of sound in a room has not yet been explored. The purpose of this study is to create a virtual source of spherical waves with TR that are of sufficient intensity to study nonlinear acoustic propagation. A parameterization study of deconvolution, one-bit, clipping, and decay compensation TR methods is performed to optimize high amplitude focusing and temporal signal focus quality. Decay compensation is introduced in this paper. Of all TR methods studied, clipping is shown to produce the highest amplitude focal signal. An experiment utilizing eight horn loudspeakers in a reverberation chamber is done with the clipping TR method. A peak focal amplitude of 9840 Pa (174 dB peak re 20 μ Pa) is achieved. Results from this experiment indicate that this high amplitude focusing is a nonlinear process.

ACKNOWLEDGMENTS

This work was made possible through the resources provided by the BYU Department of Physics and Astronomy. I would like to thank Dr. Anderson for his efforts and help throughout the process of this research. Special thanks to Sarah Young for her contributions in the experiments and data analysis.

Contents

Table of Contents	5
List of Figures	6
I. Introduction	7
II. Time Reversal Methods	9
III. Focal Signal Optimization	15
IV. High Amplitude Focusing	25
V. Conclusion	30
References	32

List of Figures

1	Impulse response signals after deconvolution, one-bit, and clipping	11
2	Impulse response signal after decay compensation.....	14
3	Photograph of setup for parameterization study.....	16
4	Results of IR length optimization study.....	19
5	Results of deconvolution optimization study.....	20
6	Comparing peak amplitude for clipping, one-bit, and decay compensation.....	23
7	Comparing temporal quality for clipping, one-bit, and decay compensation.....	24
8	Photograph of setup for high amplitude experiments	27
9	Focal signals from high amplitude experiments	30

I. Introduction

Time reversal (TR) is a signal processing technique that may be used to achieve intentional sound focusing from remotely placed sources.¹⁻² The TR process includes a forward step and a backward step. During the forward step, an impulse response (or transfer function in the frequency domain) is obtained between a source and a receiver. The impulse response is then reversed in time and additional processing may be applied at this stage. During the backward step, the reversed impulse response is broadcast from the source and a focusing of sound is achieved at the receiver location. TR has been used in biomedical applications such as lithotripsy of kidney stones and of brain tumors.³⁻⁵ Researchers optimized the strength and spatial confinement of focused waves in these applications by exploiting the complicated wave propagation in the body. It has also been used in the nondestructive evaluation of solid media, to locate and characterize cracks within a sample.⁶⁻¹⁰ Some of the applications of TR to nondestructive evaluation, such as the Time Reversed Elastic Nonlinearity Diagnostic,⁸ are similar to lithotripsy except that instead of destroying tissue with intense sound the focused waves are used to excite nonlinear signatures of cracks. Additionally, TR was used to create a high amplitude focusing of ultrasound for a noncontact source used for nondestructive evaluation.¹¹⁻¹²

This paper describes the use of TR processing to create a high amplitude focus of sound in a reverberation chamber. The purpose of these experiments is to create a virtual source of spherical waves that are of sufficient intensity to study nonlinear acoustic propagation. TR focuses waves to a selected location that converge from all directions to produce the focus, and then diverge from that location.¹³ The divergence of the waves after TR focusing may be considered a virtual source.¹⁴ To achieve the highest possible amplitude of TR focusing several

methods are explored here, including deconvolution (or inverse filtering), one-bit, clipping, and decay compensation. The comparison of these methods has not been shown to date. Decay compensation is introduced in this paper.

While the TR process has also been applied to room acoustics applications, the authors are not aware of a similar study that seeks to maximize the amplitude of the focusing of sound in a room. Yon *et al.* compared the performance of beamforming to TR focusing in a highly reverberant room with communications applications in mind.¹⁵ Candy *et al.* compared the performance of TR receivers to an optimal linear equalization receiver in extracting a transmitted signal propagating in a highly reverberant environment, with the purpose of improving communications in reverberant environments.¹⁶ Ribay *et al.* performed a time-domain, finite-difference simulation of TR in a 2-D reverberation room model, also for communications applications, in order to determine the relationship between the signal-to-noise ratio and the number of sources used in TR.¹⁷ They concluded that the focal amplitude depends on the number of physical sources, N , the length of the impulse response, and the reverberation time of the room. In another study, Candy *et al.* examined the functionality of wideband communications with TR receivers in a tunnel with many obstructions, echoes, and bends.¹⁸

This paper presents a parameterization study to optimize the TR processing methods mentioned previously for high amplitude focusing and temporal signal focus quality. The parameterization study shows that clipping is the method that produces the highest amplitude focus. A final measurement is then presented in which a TR experiment is performed with 8 loudspeaker horn sources in a reverberation chamber. A peak focal amplitude of 9840 Pa (174 dB peak re 20 μ Pa) is achieved. Results from this test indicate that this high amplitude focusing is a nonlinear process.

II. Time Reversal Methods

This section will review the basics of the deconvolution (inverse filtering), one-bit, and clipping methods and introduce the decay compensation method. Each of these methods alters the impulse response/transfer function in order to achieve improved focal amplitude or focal quality. The standard TR process involves a time reversal of the impulse response, $ir(t)$ to obtain the time reversed impulse response (TRIR), $ir(-t)$. In the standard TR process, the TRIR is broadcast from each source simultaneously to produce a focus. It should be noted here that prior to the broadcast of a TRIR or a modified TRIR, this signal is normalized to maximize the available amplification.

A. Deconvolution

Deconvolution or inverse filtering has previously been used in TR experiments to achieve a higher quality focal signal, typically at the expense of the focal amplitude.¹⁹⁻²² Tanter *et al.* found that inverse filtering reduces the amplitude of the side lobes in a TR experiment.¹⁹ The inverse filter method has also been shown to improve the retrieval of the Green's function between the source and receiver in a TR experiment, leading to a cleaner focus than one obtained via standard TR.²¹

One purpose of the deconvolution method, as outlined by Anderson *et al.*, is to obtain a delta function like focal signal.²² Thus the desired signal to broadcast during the backward step of the TR process is the frequency domain inverse of the transfer function obtained in the forward step,

$$g(\omega) = \frac{1}{R(\omega)} = \frac{R^*(\omega)}{|R(\omega)|^2} \quad (1)$$

where $g(\omega)$ is the deconvolution transfer function used to obtain focusing, $R(\omega)$ is the transfer function between the source and receiver, and $*$ denotes a complex conjugate. To avoid potentially dividing by 0 in Eq. (1), a regularization constant is added to the denominator,

$$g(\omega) = \frac{R^*(\omega)}{|R(\omega)|^2 + \gamma \text{mean}(|R(\omega)|^2)} \quad (2)$$

where γ is a unitless, regularization parameter that can be optimized to produce the cleanest focal signal. Equations (1) and (2) were given by Anderson *et al.* though similar equations were given in references 19-21. Figures 1(a) and 1(b) provide examples of an impulse response used for standard TR and an example of a signal obtained after deconvolution, respectively (the deconvolution method is applied to the standard impulse response shown in this figure with $\gamma = 0.9$). The value of γ is optimized later in this study (Anderson *et al.* used a value of $\gamma = 0.9$).

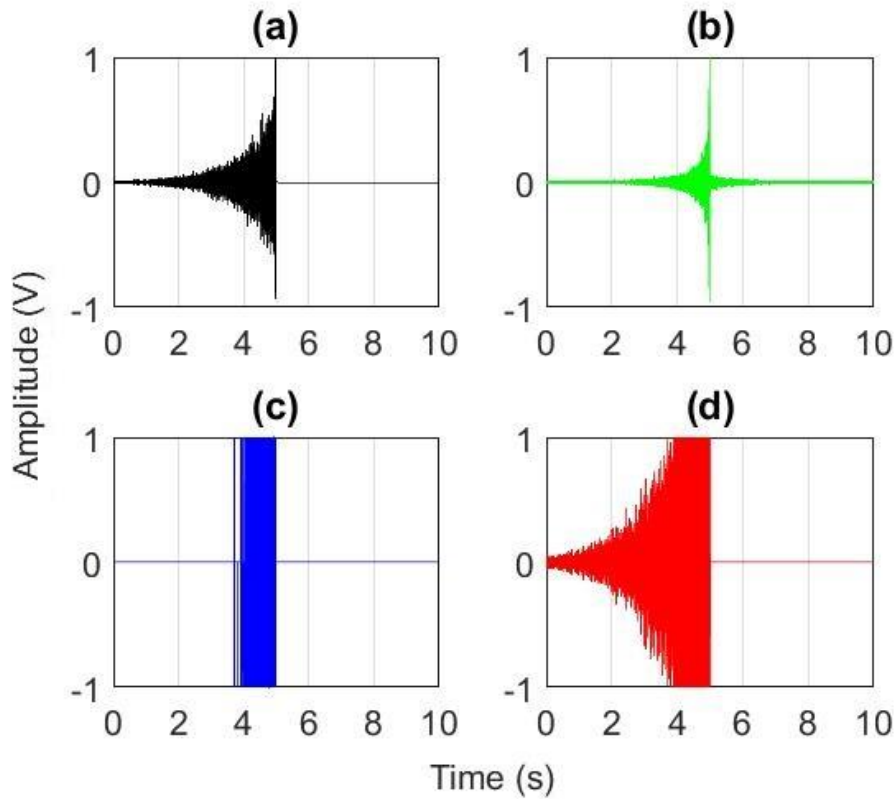


FIG. 1. (a) Standard impulse response. (b) Impulse response after deconvolution. (c) Impulse response after one-bit. (d) Impulse response after clipping.

B. One-bit

Derode *et al.* introduced the use of the one-bit method in TR experiments.²³ Their experiments in a water tank achieved an increase of 12 dB in the peak focal amplitude after implementing the one-bit method. The increase in focal amplitude was achieved at the expense of lowering the signal-to-noise ratio.

The one-bit method involves keeping only the phase information of the TRIR signal. For a normalized TRIR, a certain value between 0 and 1 is selected as a threshold and everything above the threshold gets set to +1, and everything below the negative value of the threshold gets

set to -1. For the purposes of noise rejection, everything in between the positive threshold and the negative threshold is set to 0. The resulting signal for the backward step only contains values of +1, 0, and -1. Because the phase information is preserved, the one-bit method still focuses energy. An example one-bit processed signal, with a threshold of 0.2, is shown in Fig. 1(c), with this method applied to the standard impulse response shown in this figure. The threshold value is optimized later in this study.

C. Clipping

Clipping was introduced by Heaton *et al.* as a processing method for TR that is very similar to the one-bit method.²⁴ Like the one-bit method, clipping of the normalized TRIR signal also involves a threshold value. A value between 0 and 1 is selected as a threshold and everything above the threshold gets set to +1, everything below the negative value of the threshold gets set to -1. The difference between the one-bit method and clipping is that for clipping, the signal that lies between the threshold and the negative value of the threshold remains unchanged. An example signal with clipping applied, with a threshold of 0.2, is shown in Fig. 1(d) with the clipping applied to the standard impulse response shown in this figure. The threshold value is optimized later in this study.

D. Decay Compensation

Decay compensation is a new method for TR processing. Decay compensation seeks to amplify later arrivals in a relatively long impulse response signal relative to the direct sound arrival and early reflections such that all arrivals have essentially the same amplitude. The

envelope, $e(t)$, also termed the polar energy time curve in room acoustics, of the normalized TRIR signal is obtained (through a Hilbert transform of the TRIR),

$$e(t) = \sqrt{[ir(-t)]^2 + [\hat{ir}(-t)]^2} \quad (3)$$

where $\hat{\cdot}$ represents a Hilbert transform operator.²⁵⁻²⁶ $e(t)$ may be smoothed (for each time sample, the sample and neighboring samples may be averaged). The inverse of the envelope is calculated and multiplied by the original TRIR signal to obtain the decay compensation signal, $dc(t)$,

$$dc(t) = \frac{1}{e(t)} ir(-t). \quad (4)$$

A threshold value is chosen, such that samples above the threshold (or below the negative value of the threshold) are multiplied by the inverse envelope value while samples below that threshold are unchanged. Figure 2(a) displays $e(t)$ for the $ir(-t)$ given in Fig. 2(a) with a smoothing function. The inverse of $e(t)$ is given in Fig. 2(b). $dc(t)$ is given in Fig. 2(c), with a threshold of 0.05. The threshold value is optimized later in this study.

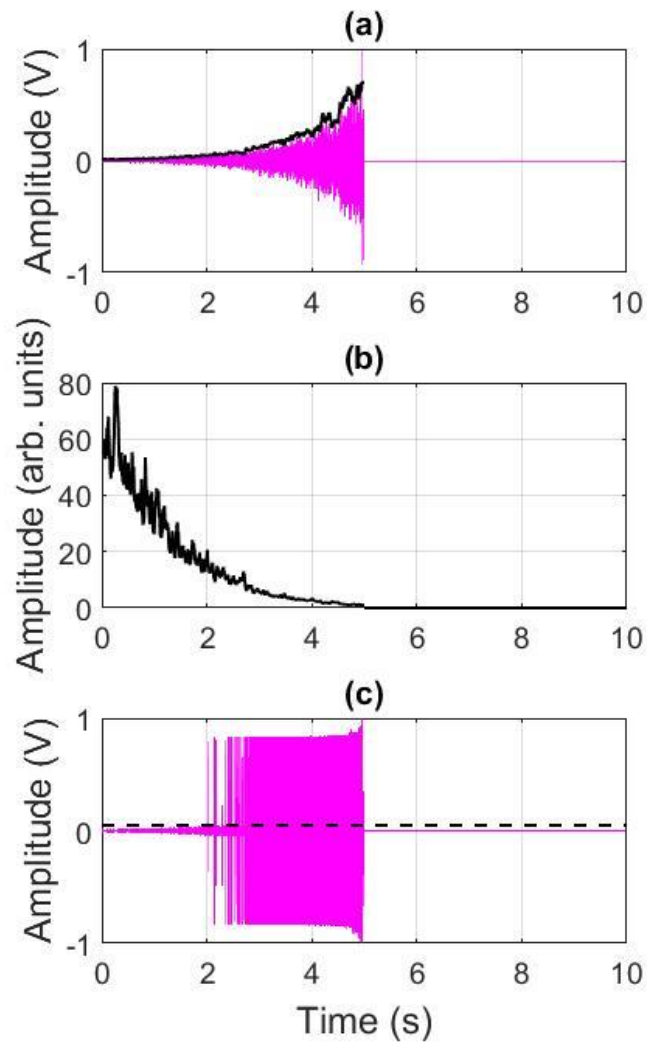


FIG. 2. (a) Envelope (black) of the impulse response signal (magenta). (b) Inverse of the envelope in (a). (c) Impulse response after applying decay compensation with the threshold value (dashed black line).

III. Focal Signal Optimization

This section describes parameterization experiments that are conducted in a reverberation chamber. The TR methods described in Section II are each optimized. The length and frequency content of the TRIR are also optimized.

A. Experimental Setup

The focal signal optimization tests are performed in a large reverberation chamber (204 m³) on the Brigham Young University campus. This room is chosen because the hard wall reflections, and therefore long reverberation time, contribute to a high amplitude focus as shown by Ribay *et al.*¹⁷ The measured reverberation time for the room was found to be 6.89 s and the Schroeder frequency of the room was determined to be 385 Hz.²⁷ All experiments are performed at frequencies above the Schroeder frequency to ensure a diffuse sound field in the chamber.

The experiments presented in this section employ a single Mackie HR824MK2 loudspeaker as the source and a 1.27 cm (1/2 inch), 46AQ GRAS random incidence microphone with a 53.03 mV/Pa sensitivity as the receiver. A random incidence microphone is chosen for the expected diffuse field in the chamber. Source signals are generated within MATLAB and broadcast from the headphone output on a Dell Latitude E4300 laptop. Data is acquired with a National Instruments PXI-4462 card, housed in a National Instruments 1042 PXI Chassis, with a 204.8 kHz sampling frequency and 24-bit resolution and a LabView program. A photograph of the experimental setup in the room is shown in Fig. 3.

Anderson *et al.* have shown that in rooms, pointing a source directly away from a receiver in a TR experiment yields the highest focal amplitude.²⁷ Thus the loudspeaker's face is pointed 180° away from the microphone. The loudspeaker's position in the room is 1.54 m from

the west wall, 1.85 m from the south wall, and 1.5 m off the ground since room acoustics standards suggest staying at least 1.5 m from any wall to best ensure a diffuse field.²⁸ Similarly the microphone is placed at least 1.5 m from any wall and is located 1.65 m from the north wall, 1.59 m from the east wall, and 1.61 m off the ground. The distance between the speaker and the microphone is 3.18 m.

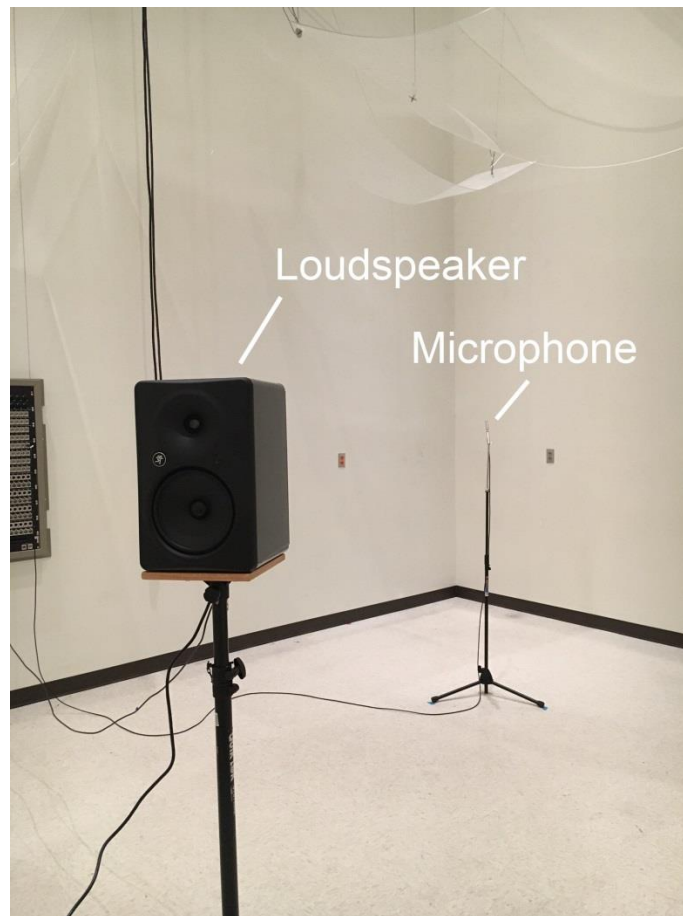


FIG. 3. Photograph of the setup used in the optimization experiments in the reverberation chamber.

The source signal, $s(t)$, in the forward step is a logarithmic chirp signal. The pressure response, $r(t)$, is recorded at the microphone. The recording time is set for 10 s to be long enough to exceed the reverberation time. A cross-correlation between $s(t)$ and $r(t)$ is used to estimate the impulse response, $ir(t)$.²⁷ Depending on the particular experiment, additional processing to implement deconvolution, one-bit, etc. is then applied at this stage to the normalized $ir(t)$. The TRIR was then broadcast from the loudspeaker to produce a focus at the microphone location.

B. Optimization Metrics

The peak amplitude and temporal quality are two metrics used here to characterize the focal signal. Peak amplitude, A_p , is a measure of the maximum pressure magnitude (in Pa) achieved in the focal signal. Temporal quality, defined by Heaton *et al.*, compares the squared peak focal amplitude to the average squared pressure present in the signal.²⁴ Because these experiments involve discrete time signals, the following adapted equation is used to calculate the temporal quality,

$$\xi_T = \sqrt{\frac{[A_p]^2}{\frac{1}{N} \sum_{n=0}^N [A(x_0, y_0, z_0, n)]^2}} \quad (5)$$

where N is the length of the signal in samples, and $A(x_0, y_0, z_0, n)$ is the amplitude of the n th sample at the microphone focal position (x_0, y_0, z_0) . ξ_T is a unitless metric that, with the square root, effectively gives a ratio of peak amplitude to the average pressure magnitude throughout the signal. A delta function signal would have $\xi_T = \sqrt{N}$, a sine wave signal would have $\xi_T = \sqrt{2}$, and a random noise signal would have $\xi_T = \sqrt{3}$.

C. Results of Optimization Experiments

A total of six sets of optimization experiments are conducted to optimize the TRIR processing: source bandwidth, impulse response length, deconvolution, one-bit, clipping, and decay compensation.

The source bandwidth is varied to determine the bandwidth of the chirp signal that will maximize A_p for standard TR. Thirty-three different bandwidths are tested ranging from 500 Hz to 16 kHz. Frequencies below 500 Hz are not examined due to the Schroeder frequency limit of 385 Hz. The reverberation time in rooms is typically smaller for high frequencies than for low frequencies, thus higher frequency content may not contribute much to TR focusing. The only variable changed in this experiment is the bandwidth of the initial chirp signal, $s(t)$. The first experiment is done over a bandwidth of 7 kHz to 8 kHz, and the subsequent experiments include more frequency content until a bandwidth of 500 Hz to 16 kHz is reached. The experiments show that adding higher frequency content generally improves ξ_T of the focal signal, while adding lower frequency content degrades ξ_T . However, it is also found that adding lower frequency content does more to boost A_p of the resulting focal signal. The band from 500 Hz to 9500 Hz produced the highest A_p of 17.2 Pa and a ξ_T of 93.3. The rest of the sets of optimization experiments are performed with the optimal 500 Hz to 9500 Hz band.

The length of the impulse response using standard TR is varied to determine the minimum length of the impulse response needed before A_p is maximized. A nearly 5 s long TRIR is obtained and prior to the broadcast of the TRIR from the loudspeaker, the length of the TRIR was changed. A total of 7 different TRIR lengths were tested, ranging from 0.5 s to the full TRIR length of 4.97 s. The results in Fig. 4 show that shortest length to achieve maximal A_p is around 2.0 s. The minimum length needed in a given room likely depends on the reverberation

time in that room. These results confirm those found by Ribay *et al.*, that the length of the impulse response affects A_p .¹⁷

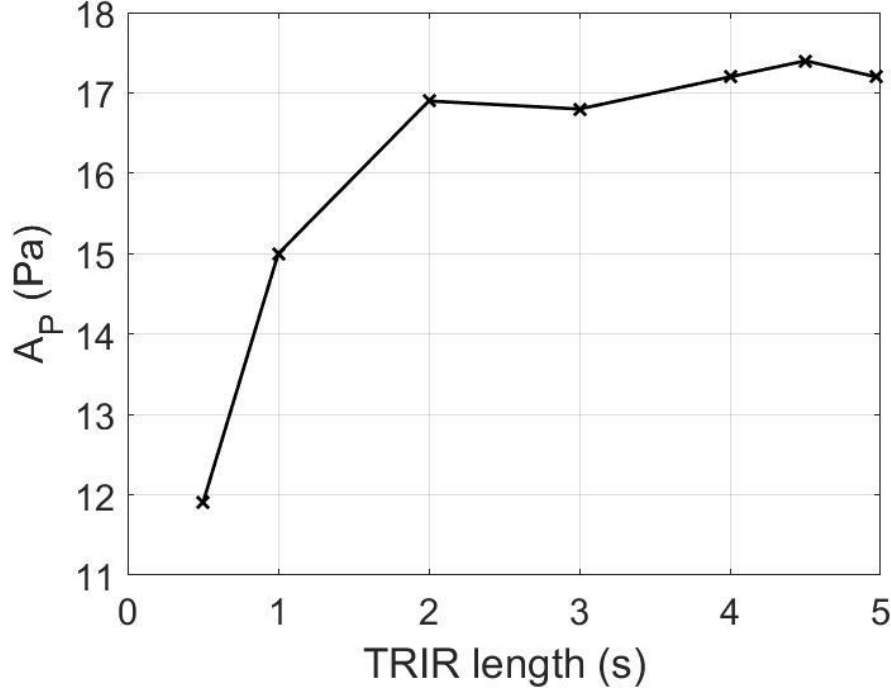


FIG. 4. Peak focal amplitude of a standard time reversal experiment as a function of the length of the impulse response used.

The experiments optimizing deconvolution are done by obtaining a TRIR and then changing the γ parameter in the deconvolution processing (see Eq.(2)) before broadcasting the modified TRIR from the loudspeaker. One-hundred, logarithmically-spaced γ values are tested, ranging from 10^{-6} to 10^3 . The modified TRIR signal is then broadcast from the loudspeaker and a focal signal is recorded at the microphone for each of the 100 γ values. The results of the deconvolution experiments are shown in Fig. 5. As γ approaches infinity, the deconvolution processing becomes equivalent to standard TR since the magnitude squared term in the

denominator of Eq. (2) is small compared to the very large γ term. The modified TRIR is then normalized and Eq. (2) becomes just a standard TRIR. A γ value of zero results in an amplification of noise and therefore a low ξ_T . As described earlier in this section in the literature, deconvolution produces signals with higher ξ_T (ξ_T is related to the signal to noise ratio used in the literature) at the expense of a reduction in A_P .

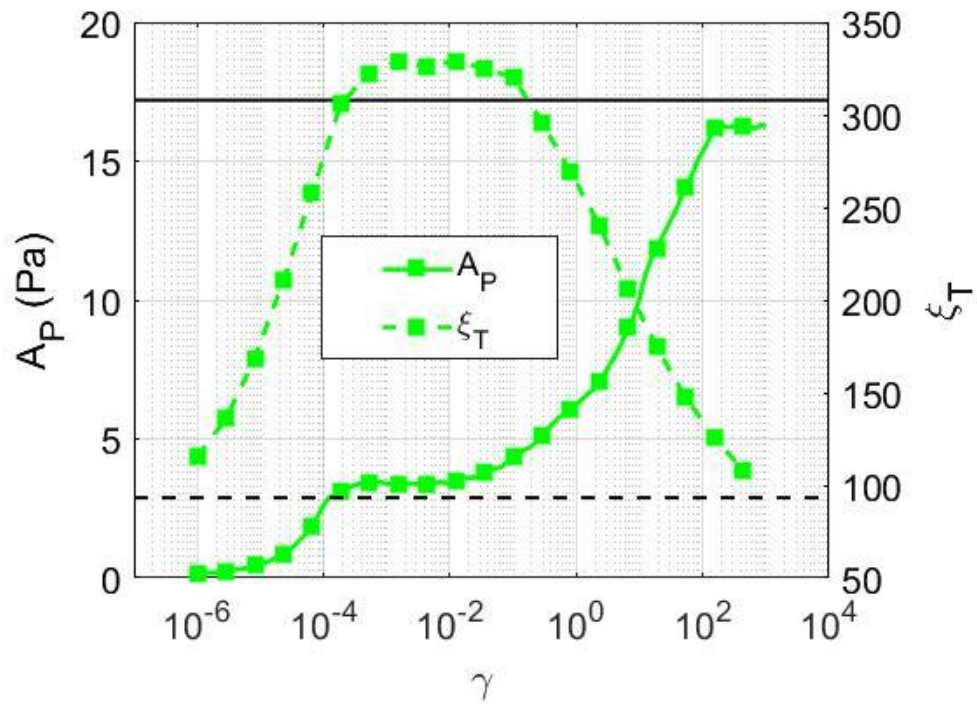


FIG. 5. Results of the optimization of deconvolution processing. The focal amplitude, A_P , (solid line) and the temporal quality, ξ_T , (dashed line) are each plotted as a function of the regularization parameter, γ . The solid black line represents the A_P for standard TR, and the dashed black line represents the ξ_T for standard TR.

Since the purpose of using deconvolution is to produce focal signals with higher ξ_T , and no value of γ results in a higher A_P than using standard TR, the optimum γ value of 0.1 is selected. This value differs from the γ value of 0.9 given by Anderson *et al.*²² The optimal value for γ may well depend on the available signal to noise ratio in the system. Gamma values below 0.1 do not produce focal signals with significantly higher ξ_T , and ξ_T begins to decrease with γ values larger than 0.1. Smaller γ values could be used at the expense of further reductions in A_P . A γ value of 0.1 produced a focal signal with $A_P = 4.4$ Pa and $\xi_T = 320$. Compared to standard TR, the optimal deconvolution focal signal has a ξ_T that is 3.43 times greater, but a A_P that is 3.91 times lower. For the purposes of maximizing A_P , the significant amplitude reduction does not make deconvolution the optimal technique for producing a high amplitude focus.

In the optimization of the one-bit, clipping, and decay compensation signal processing methods, the threshold value is the parameter modified to find the optimum value for high amplitude focusing. Section II described the manner in which the threshold is applied for these methods. For each of these experiments, a TRIR signal is obtained, processed according to the method employed, and then broadcast from the loudspeaker to achieve a focus at the microphone. One-hundred, logarithmically-spaced threshold values are tested for each processing method, ranging from 10^{-5} to 1.

The results of the one-bit, clipping, and decay compensation sets of experiments are shown in Figs. 6 and 7. Figure 6 compares A_P for the three methods, and Fig. 7 compares ξ_T for the three methods. These results show that decreasing the threshold value generally creates focal signals with a higher A_P for all three types of signal processing. Also, the increase in A_P is gained generally at the expense of decreasing ξ_T .

Of the three processing methods, clipping produces the highest A_p . This makes sense since more energy is broadcast when clipping is used because the low amplitude samples are not zeroed out as they are in one-bit processing. The optimum clipping threshold value of 0.03 produces a focal signal with $A_p = 110.8$ Pa. This means that with the optimum clipping threshold, the A_p of a standard TR focal signal of 17.2 Pa can be amplified by a factor of 6.44. In terms of dB, clipping processing produces a gain of 16.2 dB. There is a decrease in ξ_T , from 93.3 with standard TR down to 72.9 with clipping processing, a 21.9% reduction. The drop in ξ_T is offset by the significant gain in A_p .

The decay compensation method performs better than the one-bit method both in terms of A_p and ξ_T across nearly every threshold value. The optimum threshold value for decay compensation is found to be 0.005. This optimum threshold for decay compensation produced a focal signal with $A_p = 88.5$ Pa and $\xi_T = 61.9$. The A_p of 88.5 Pa is 5.15 times greater than the A_p for standard TR, but it is accompanied with a 33.7% reduction in ξ_T . The optimum threshold value for the one-bit method is found to be 0.02. This optimum threshold for the one-bit method produced a focal signal with $A_p = 78.7$ Pa and $\xi_T = 63.5$. The A_p of the optimal one-bit focal signal is 4.58 times greater than the A_p for standard TR, but ξ_T is 31.9% less than ξ_T achieved with standard TR.

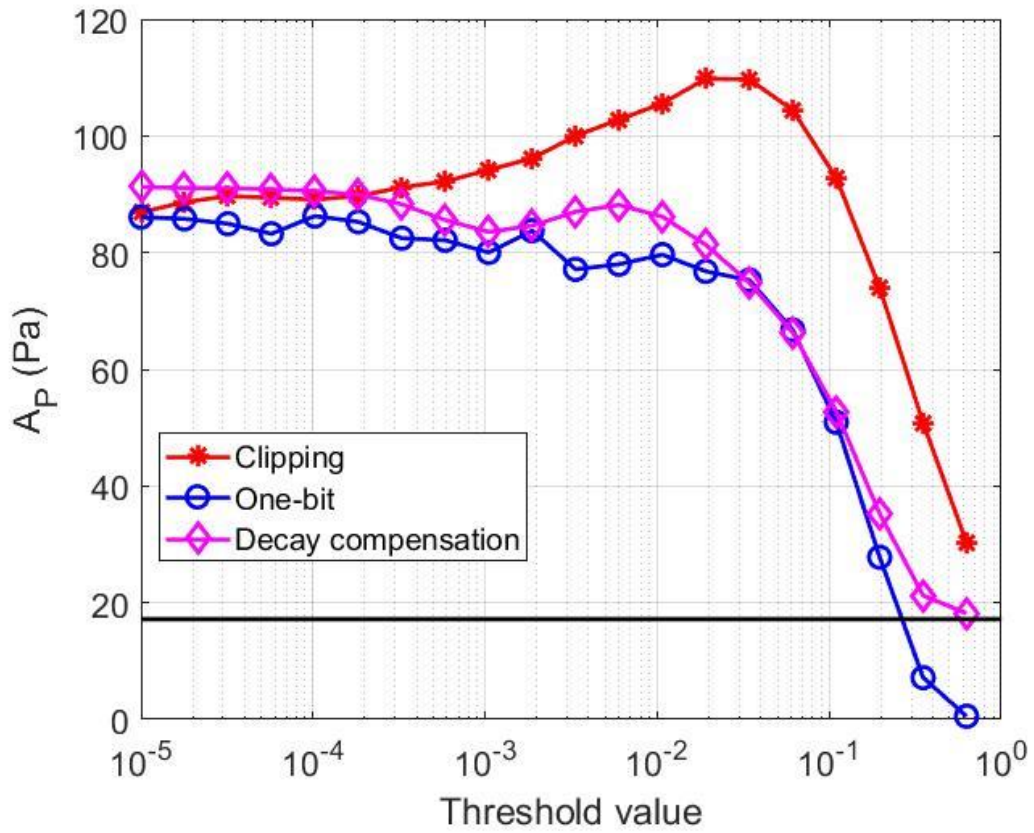


FIG. 6. Comparison of the peak focal amplitude, A_p , of the clipping, one-bit, and decay compensation methods over 100 threshold values. The solid black line represents the A_p for standard TR.

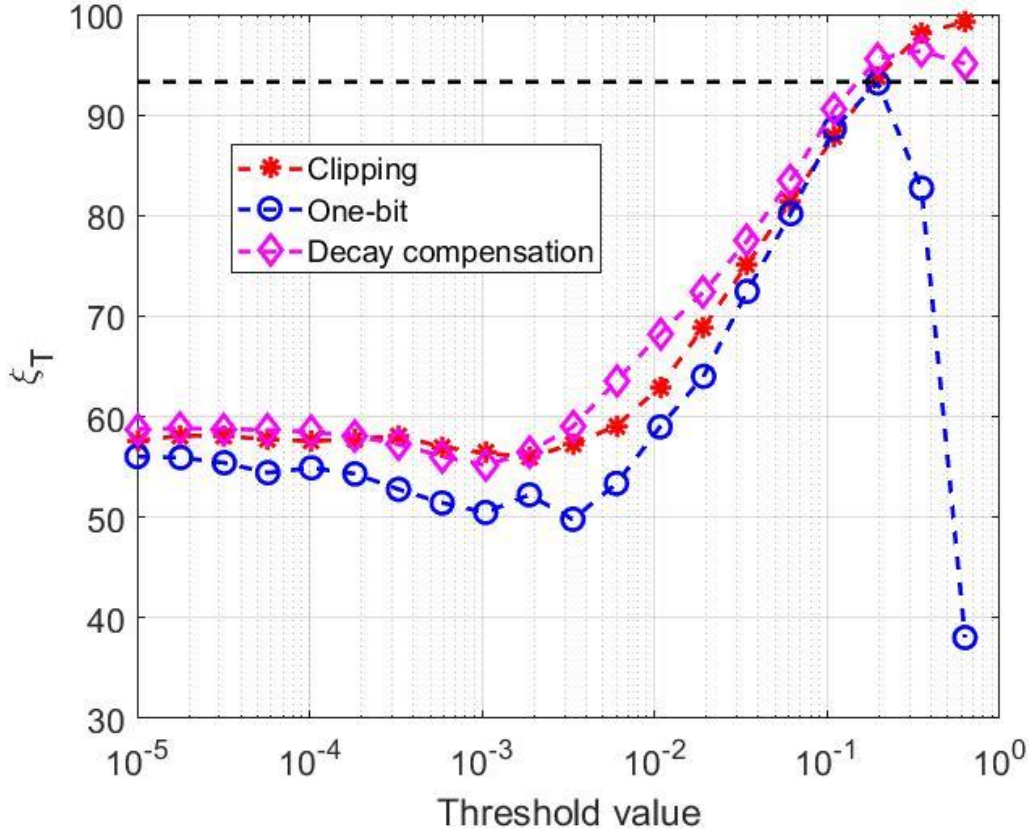


FIG. 7. Comparison of the temporal quality, ξ_T , of the clipping, one-bit, and decay compensation methods over 100 threshold values. The dashed black line represents the ξ_T for standard TR.

Though not presented here in detail, the clipping, one-bit, and decay compensation methods are applied to the deconvolution modified TRIR signals. The results indicate that both ξ_T (inherited from the deconvolution) and A_p (inherited from the clipping, one-bit, and decay compensation) of the focusing improve compared to standard TR. For clipping with deconvolution, the optimum threshold value is 0.01, slightly lower than the optimum threshold of 0.03 for clipping with standard TR. The optimum threshold for clipping with deconvolution produces a focal signal with $A_p = 43.5$ Pa and $\xi_T = 162.2$. Compared to standard TR, A_p

increases by a factor of 2.5 and ξ_T increases by a factor of 1.7. This increase in both A_P and ξ_T shows the robustness of combining deconvolution with clipping techniques to achieve better focusing than standard TR. However the reduction in A_P , relative to when deconvolution is not used, is a drawback to using deconvolution and clipping, for example, to achieve the highest possible focusing amplitude.

Before the high amplitude experiments are conducted, a seventh optimization experiment is done to determine the best placement of the sources to achieve the highest possible amplitude for TR focusing. Experiments are conducted with a microphone in the same location as it was in the other optimization experiments (on a stand, 1.61 m off the ground). The loudspeaker is moved to different locations in the room, and a standard TR experiment is done at each location to determine optimum speaker placement for the highest amplitude focus. The results show that the highest amplitude is achieved when the speaker and the microphone are in the same horizontal plane (the primary axis of the loudspeaker is directed in the plane of the microphone), and when the loudspeaker and microphone are placed in corners of the room.

IV. High Amplitude Focusing

Building off the results of the previous section, a new experiment is designed to achieve the highest possible focusing amplitude by using the optimal processing of the TRIR, more efficient sound sources, and a larger N . The high amplitude focusing measurements are performed in the same reverberation chamber as the optimization experiments. The setup consists of eight BMS 4590 coaxial compression drivers with horns attached to the drivers. Two 0.3175 cm (1/8 inch) GRAS free-field microphones are used for these measurements. Random incidence microphones are unavailable for this size microphone. One microphone is used as the

target microphone (the microphone being focused to), and the other is used as an away microphone to get the response from another location in the room away from the focal position. The target microphone has a sensitivity of 0.76 mV/Pa, and the away microphone has a sensitivity of 1.01 mV/Pa. Both microphones have a specified upper limit on their dynamic range of 175 dB for a ± 1 dB precision.

The signals used for these experiments are created in MATLAB and output via two, 4-channel Spectrum M2i.6022-exp generator cards. The acquisition is done with one, 4-channel Spectrum M2i.4931-exp digitizer card. A sampling frequency of 30 MHz is used and the digitizer has 16 bit precision. The output from the Spectrum cards is amplified with two, 4-channel Crown CT4150 amplifiers. The amplified signal is routed through patch panels via Speakon cables into the reverberation chamber and then to the horn drivers. A panoramic photograph of the setup for the high amplitude focusing experiments is shown in Fig. 8.

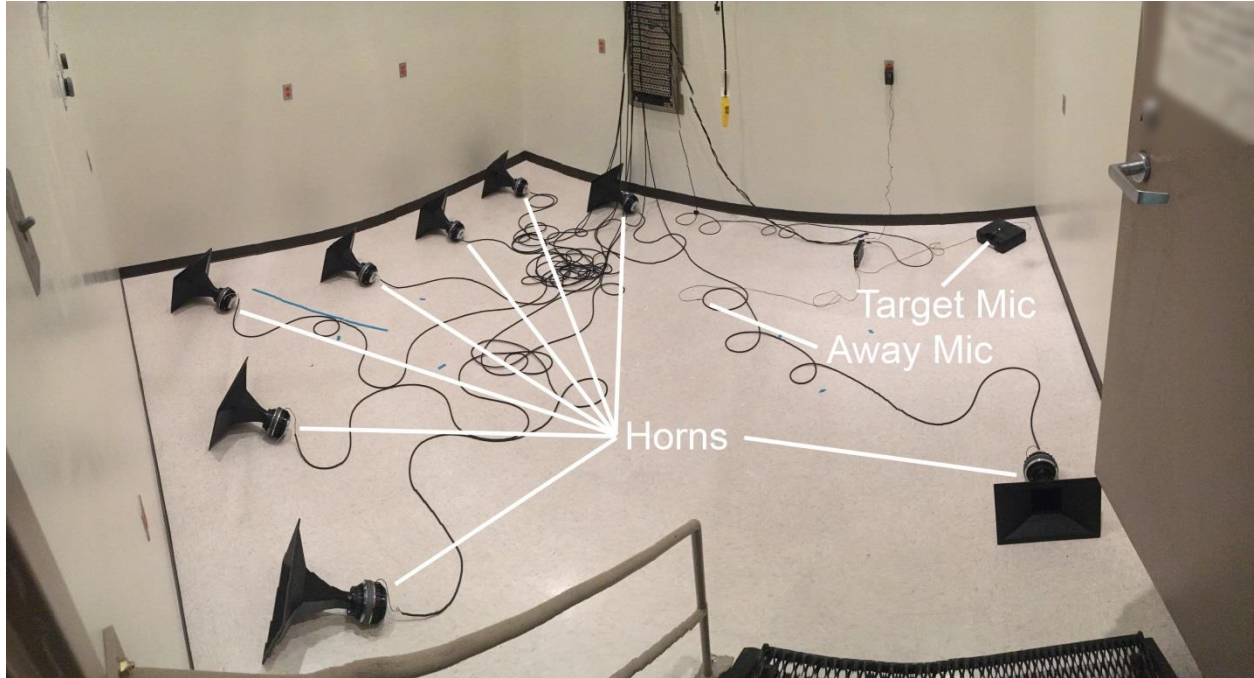


FIG. 8. Panoramic photograph of the high amplitude focusing experimental setup in the reverberation chamber.

Based on the results of the optimization experiments, the drivers are placed close to the corners of the room or close to the adjoining boundary of a wall and the floor. The orientation of each driver is facing 180° away from the target microphone. The target microphone is placed near a corner in the room in order to achieve the highest possible A_p .

Due to constraints on the upper frequency limit of the mid-range coaxial compression driver, the bandwidth of the initial chirp signal is 500 Hz to 7000 Hz. This is not a significant issue in terms of amplitude reduction however, because in the earlier optimization experiments the difference in A_p is minimal between the optimal bandwidth of 500 Hz to 9500 Hz and the bandwidth of 500 Hz to 7000 Hz.

A first experiment is performed to compare the clipping method to standard TR at a much higher amplitude than the experiments done in Section III. For consistency in comparing the results of the clipping experiment to standard TR, the same amplification settings are used for both measurements. The Crown amplifiers are set to zero attenuation and the output voltage on the Spectrum M2i.6022-exp generator cards is set to 1 V. The first measurement performed is a standard TR measurement. This measurement produces a focal signal with $A_p = 1220$ Pa (156 dB peak) and $\xi_T = 146.5$. A measurement is then performed with the clipping method. Clipping produces a focal signal with $A_p = 6730$ Pa (171 dB peak) and $\xi_T = 106.2$. Thus clipping increases A_p by a factor of 5.5 or an increase of 14.8 dB, which is similar to the 16.2 dB gain found in the optimization experiments in Section III. As expected, clipping is able to produce a higher amplitude focus than standard TR. The addition of more sources, that are each capable of a higher sound level output, increases not only A_p but also ξ_T of the focal signal with both standard TR and clipping, as expected.

In order to observe whether the TR focusing at these amplitudes is a linear or a nonlinear process, six experiments are performed with the clipping method. One is done at a low amplitude, one is done at a high amplitude, and the others are done at intermediate amplitudes. For the lowest amplitude case (Level 1) the input attenuation knobs on the Crown amplifiers are set to 75% of their maximum attenuation with the output voltage on the Spectrum M2i.6022-exp generator cards set to 1 V. For the intermediate cases (Levels 2-5) the input attenuation knobs on the Crown amplifiers are set to 50%, 25%, 0%, and 0% of their maximum attenuation with the output voltage on the Spectrum M2i.6022-exp generator cards set to 1 V, 1 V, 1 V, and 1.5 V, respectively. For the highest amplitude case (Level 6) the input attenuation knobs on the Crown amplifiers are set to zero attenuation with the output voltage on the Spectrum M2i.6022-exp

generator cards set to 2 V. If the focusing is a linear process then the low amplitude focal signals should be identical to the highest amplitude focal signal when scaled appropriately, aside from background noise.

The lowest amplitude experiment produces a focal signal with $A_p = 589$ Pa (149 dB peak). The highest amplitude experiment produces a focal signal with $A_p = 9840$ Pa (174 dB peak). The lowest and intermediate amplitude signals are scaled upwards until the early arrivals of the low and high amplitude signals match. Scaling according to the early arrivals is done because the exact amplification increase as the amplifier knobs are turned up is not precise. Also, the portion of the signal before the focal time should be at a lower amplitude and be more likely to scale linearly. The scaled lowest amplitude result is compared with the highest amplitude result in Fig. 9(a) and all six amplitude level results are compared in Fig. 9(b). Figure 9(a) shows the scaled low amplitude measurements matching the highest amplitude case well before and well after the time of focusing. Figure 9(b) shows the comparison between the scaled lowest amplitude and intermediate amplitude cases and the highest amplitude case at the time of focusing. The portions of the signals before the time of peak focusing scale fairly linearly. At times just prior, at, and just after the time of peak focusing these two signals do not scale linearly (as seen in Fig. 9(b)). The A_p of the highest amplitude signal is less than the A_p of the scaled lowest amplitude signal by a factor of 1.29. As the amplified signals sent to the horns are increased, the nonlinearity of the focusing process becomes more evident (the amplitudes depart further and further from the lowest amplitude setting).

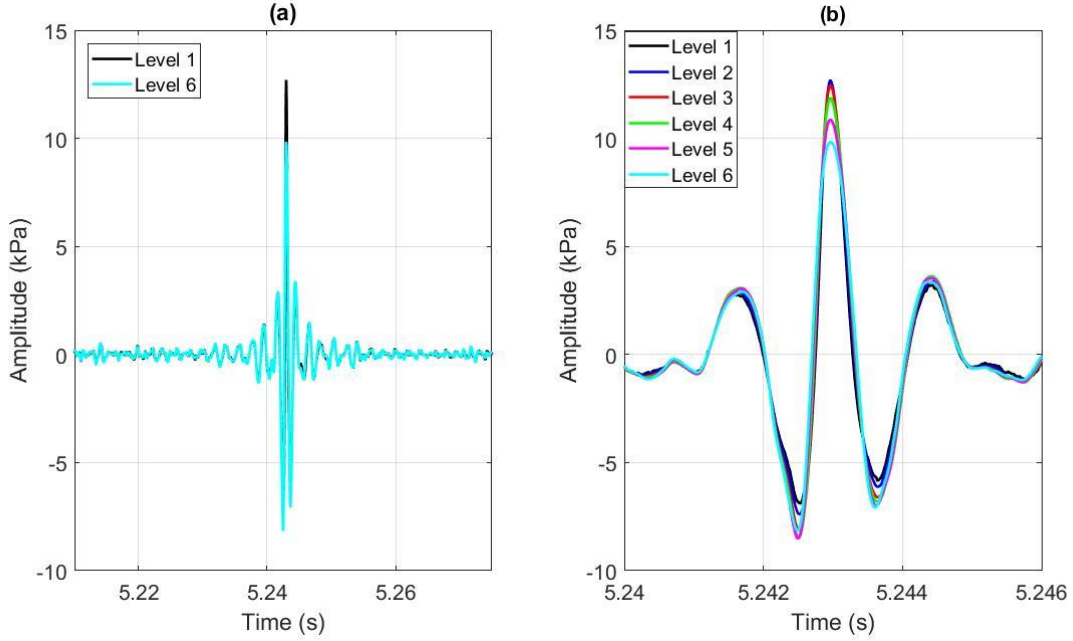


FIG. 9. Focal signals obtained from the clipping TR method at high amplitudes. (a) The scaled lowest amplitude (Level 1) and highest amplitude (Level 6) signals are shown. (b) The scaled lowest amplitude, intermediate amplitude (Levels 2-5), and highest amplitude signals are shown.

V. Conclusion

A parameterization study has been presented, seeking to optimize the peak amplitude, A_P , of time reversal (TR) focusing and the temporal quality, ξ_T , of the TR focal signals for deconvolution, one-bit, clipping, and decay compensation TR methods. Decay compensation is a new method presented here that seeks to amplify later arrivals in an impulse response signal so that all arrivals essentially have the same amplitude. This method performed better than the one-bit method both in terms of focal amplitude, A_P , and temporal quality, ξ_T . The optimal regularization parameter, γ , value was found for the deconvolution method, and optimal

threshold values were found for the clipping, one-bit, and decay compensation methods. It has been shown that the clipping method is the TR method that produces the highest amplitude focus of sound in a reverberation chamber.

With eight horn loudspeaker sources in a reverberation chamber and the optimal clipping threshold, $A_p = 9840$ Pa (174 dB peak) was achieved. Experiments conducted at lower amplitudes and scaled appropriately to the highest amplitude result provide evidence that TR focusing at these high amplitudes is a nonlinear process.

References

- ¹ M. Fink, "Time reversed acoustics," *Phys. Today* **50**(3), 34-40 (1997).
- ² B. E. Anderson, M. Griffa, C. Larmat, T. J. Ulrich, and P. A. Johnson, "Time reversal," *Acoust. Today* **4**(1), 5-16 (2008).
- ³ J.-L. Thomas, F. Wu, and M. Fink, "Time reversal mirror applied to lithotripsy," *Ultrason. Imag* **18**, 106–121 (1996).
- ⁴ J.-L. Thomas and M. Fink, "Ultrasonic beam focusing through tissue inhomogeneities with a time reversal mirror: application to transskull therapy," *IEEE Trans. Ultrason. Ferroelect. Freq. Contr.* **43**(6), 1122–1129 (1996).
- ⁵ M. Tanter, J.-L. Thomas, and M. Fink, "Focusing and steering through absorbing and aberating layers: application to ultrasonic propagation through the skull," *J. Acoust. Soc. Am.* **103**(5), 2403–2410 (1998).
- ⁶ C. Prada, E. Kerbrat, D. Cassereau, and M. Fink, "Time reversal techniques in ultrasonic nondestructive testing of scattering media," *Inv. Prob.* **18**, 1761-1773 (2002).
- ⁷ E. Kerbrat, C. Prada, D. Cassereau, and M. Fink, "Ultrasonic nondestructive testing of scattering media using the decomposition of the time reversal operator," *IEEE Trans. Ultrason. Ferroelectr. Freq. Control.* **49**, 1103–13 (2002).
- ⁸ T. J. Ulrich, P. A. Johnson, and A. Sutin, "Imaging nonlinear scatterers applying the time reversal mirror," *J. Acoust. Soc. Am.* **119**(3), 1514-1518 (2006).
- ⁹ B. E. Anderson, M. Griffa, T. J. Ulrich, P.-Y. Le Bas, R. A. Guyer, and P. A. Johnson, "Crack localization and characterization in solid media using time reversal techniques," *Am. Rock Mech. Assoc.*, #10-154 (2010).
- ¹⁰ B. E. Anderson, L. Pieczonka, M. C. Remillieux, T. J. Ulrich, and P.-Y. Le Bas, "Stress corrosion crack depth investigation using the time reversed elastic nonlinearity diagnostic," *J. Acoust. Soc. Am.* **141**(1), EL76-EL81 (2017).
- ¹¹ P.-Y. Le Bas, T. J. Ulrich, B. E. Anderson, and J. J. Esplin, "A high amplitude, time reversal acoustic non-contact excitation (TRANCE)," *J. Acoust. Soc. Am.* **134**(1), EL52-EL56 (2013).
- ¹² P.-Y. Le Bas, M. C. Remillieux, L. Pieczonka, J. A. Ten Cate, B. E. Anderson, and T. J. Ulrich, "Damage imaging in a laminated composite plate using an air-coupled time reversal mirror," *Appl. Phys. Lett.* **107**, 184102 (2015).

- 13 B. E. Anderson, T. J. Ulrich, and P.-Y. Le Bas, “Comparison and visualization of the focusing wave fields of various time reversal techniques in elastic media,” *J. Acoust. Soc. Am.* **134**(6), EL527-EL533 (2013).
- 14 M. Scalerandi, A. S. Gliozzi, B. E. Anderson, M. Griffa, P. A. Johnson, and T. J. Ulrich, “Selective source reduction to identify masked sources using time reversal acoustics,” *J. Phys. D Appl. Phys.* **41**, 155504 (2008).
- 15 S. Yon, M. Tanter, and M. Fink, “Sound focusing in rooms: the time-reversal approach,” *J. Acoust. Soc. Am.* **113**(3), 1533-1543 (2003).
- 16 J. V. Candy, A. W. Meyer, A. J. Poggio, and B. L. Guidry, “Time-reversal processing for an acoustic communications experiment in a highly reverberant environment,” *J. Acoust. Soc. Am.* **115**(4), 1621-1631 (2004).
- 17 G. Ribay, J. de Rosny, and M. Fink, “Time reversal of noise sources in a reverberation room,” *J. Acoust. Soc. Am.* **117**(5), 2866-2872 (2005).
- 18 J. V. Candy, D. H. Chambers, C. L. Robbins, B. L. Guidry, A. J. Poggio, F. Dowla, and C. A. Hertzog, “Wideband multichannel time-reversal processing for acoustic communications in a tunnel-like structure,” *J. Acoust. Soc. Am.* **120**(2), 838-851 (2006).
- 19 M. Tanter, J.-L. Thomas, and M. Fink, “Time reversal and the inverse filter,” *J. Acoust. Soc. Am.* **108**(1), 223-234 (2000).
- 20 M. Tanter, J.-F. Aubry, J. Gerber, J.-L. Thomas, and M. Fink, “Optimal focusing by spatio-temporal filter. I. basic principles,” *J. Acoust. Soc. Am.* **110**(1), 37-47 (2001).
- 21 T. Gallot, S. Catheline, P. Roux, and M. Campillo, “A passive inverse filter for Green’s function retrieval,” *J. Acoust. Soc. Am.* **131**(1), EL21–EL27 (2011).
- 22 B. E. Anderson, J. Douma, T. J. Ulrich, and R. Snieder, “Improving spatio-temporal focusing and source reconstruction through deconvolution,” *Wave Motion* **52**(9), 151-159 (2015).
- 23 A. Derode, A. Tourin, and M. Fink, “Ultrasonic pulse compression with one-bit time reversal through multiple scattering,” *J. Appl. Phys.* **85**(9), 6343-6352 (1999).
- 24 C. Heaton, B. E. Anderson, and S. M. Young, “Time reversal focusing of elastic waves in plates for an educational demonstration,” *J. Acoust. Soc. Am.* **141**(2), 1084-1092 (2017).
- 25 J. Vanderkooy and S. P. Lipschitz, “Uses and abuses of the energy-time curve,” *J. Audio Eng. Soc.* **38**(11), 819–836 (1990).

- ²⁶ J. J. Esplin, B. E. Anderson, T. W. Leishman, and B. T. Thornock, “The effects of non-cardioid directivity on incidence estimation using the polar energy time curve,” *J. Acoust. Soc. Am.* **130**(4), EL244-EL250 (2011).
- ²⁷ B. E. Anderson, M. Clemens, and M. L. Willardson, “The effect of transducer directionality on time reversal focusing,” *J. Acoust. Soc. Am.* **142**(1), EL95-EL101 (2017).
- ²⁸ ISO 3741:2010, *Acoustics-Determination of sound power and sound energy levels of noise sources using sound pressure – Precision methods for reverberation test rooms* (International Organization for Standardization, Geneva, Switzerland, 2010).